Available online at www.sciencedirect.com
ScienceDirect
Trans. Nonferrous Met. Soc. China 23(2013) 2496−2501
Transactions of Nonferrous Metals Society of China
www.tnmsc.cn

# Microstructure evolution of 3003/4004 clad ingots under diverse physical fields

Ying FU, Jin-chuan JIE, Yu-bo ZHANG, De-shui ZHONG, Ji-zhan LI, Ting-ju LI

School of Materials Science and Engineering, Dalian University of Technology, Dalian 116024, China

Received 9 July 2012; accepted 30 December 2012

**Abstract:** In order to improve the quality of clad ingots, diverse physical fields including electromagnetic stirring, power ultrasonic and compound field of ultrasonic and electromagnetic stirring were attempted to prepare clad ingots of 3003/4004 alloys. The solidification structures near the interface in clad ingots were investigated. The experiment results indicate that the solidification structure of 4004 alloy changes from dendritic crystals to petal-like grains when the clad ingot is treated by electromagnetic stirring. With the effect of power ultrasonic, the solidified microstructure of 4004 alloy exhibits the refinement of both primary $\alpha$(Al) and eutectic silicon. Under the compound field, the primary $\alpha$(Al) is refined, the morphology of eutectic silicon has a transition from a coarse plate-like form without treatment or thin acicular-like form with power ultrasonic to fine coral-like form.

**Key words:** Al alloy; clad ingot; power ultrasonic; electromagnetic stirring; compound field; structure

## 1 Introduction

Clad ingots, also called bimetallic ingots, consist of layers of two or more different materials. These materials have been widely used in many industrial fields due to their unique properties which cannot be obtained from a monolithic material [1]. In recent years, many methods of producing clad ingots have been developed. These involve roll bonding [2], explosive welding [3], diffusion bonding [4], extrusion clad [5], spray deposition technique [6] and casting [7]. The casting method for production of clad ingots is more efficient and economical than other processes. Therefore, this method has drawn great attention by many researchers in recent years.

In this work, a semi-continuous casting method was developed to prepare clad ingot. The bimetal slab of 3003/4004 alloy (442 mm×128 mm×1000 mm) was successfully prepared [8]. In order to improve the quality of clad ingots, diverse physical fields were used for the production of aluminum alloy clad ingots. Static test method was employed (i.e. solid−liquid bonding method) to simulate the process of continuous casting and produce aluminum alloy clad ingots.

## 2 Experimental

In this experiment, 3003 aluminum alloy is the outer layer material, and 4004 aluminum alloy is the inner layer material. The chemical compositions of experimental materials are given in Table 1. The experimental setups consist of power ultrasonic and electromagnetic stirring equipment, temperature measurement system, and two resistance furnaces.

The schematic diagram of experimental procedure is shown in Fig. 1. For step 1, 3003 alloy melt is poured into the steel mold with 52 mm in diameter and 70 mm in height. For step 2, after 20 s, the 3003 alloy melt forms a solidified shell, and the residual 3003 melt is poured out. For step 3, 4004 alloy melt is poured into the solidified shell of 3003 alloy, after that, for step 4, the solidification shell of 3003 alloy with 4004 melt is moved into electromagnetic stirring coil, and the diverse physical fields are imposed till the end of solidification process. The detail experimental parameters are shown in Table 2. In the end, the solidified ingots (70 mm in height, 50 mm in diameter) are obtained, which are cut along the central horizonal plane, ground and polished for macro and micro-metallographic examination. The

**Foundation item:** Project (51074031) supported by the National Natural Science Foundation of China; Project supported by the Korea National Project
**Corresponding author:** Ting-ju LI; Tel/Fax: +86-411-84708940; E-mail: tjuli@dlut.edu.cn
DOI: 10.1016/S1003-6326(13)62760-0

**Table 1** Chemical composition of experimental alloys (mass fraction, %)

| Alloy | Si | Fe | Cu | Mn | Mg | Zn | Al |
|---|---|---|---|---|---|---|---|
| 3003 | 0.6 | 0.7 | 0.05−0.20 | 1.0−1.5 | − | 0.10 | Bal. |
| 4004 | 9.0−10.5 | 0.8 | 0.25 | 0.10 | 1.0−2.0 | 0.20 | Bal. |

proportion of etching agent is 75 mL HCl, 25 mL $HNO_3$ and 5 mL HF. The solution of 0.5% HF is used as microstructure etching agent.

## 3 Results and discussion

### 3.1 Effect of physical fields on solidification structures of bimetal interface

The macrostructures of clad ingots are shown in Fig. 2. From Fig. 2(a), it can be obviously seen, under as-cast condition, the developed columnar crystals grow from the interface towards the inner alloy side, which parallels the heat flow but in the opposite direction, and in the center of 4004 alloy, there are coarse equiaxed grains. Under the effect of electromagnetic stirring, the solidification structure of inner 4004 alloy changes from columnar grains to equiaxed grains, as shown in Fig. 2(b). Figure 2(c) shows the ingot treated by power ultrasonic. The results indicate that the solidification structure of inner alloy transforms from coarse columnar crystals to fine equiaxed grains. The similar refinement results can be found in the ingot under compound field, as shown in Fig. 2(d).

The samples were taken from different positions near the interface in the ingots, as shown in Fig. 3.

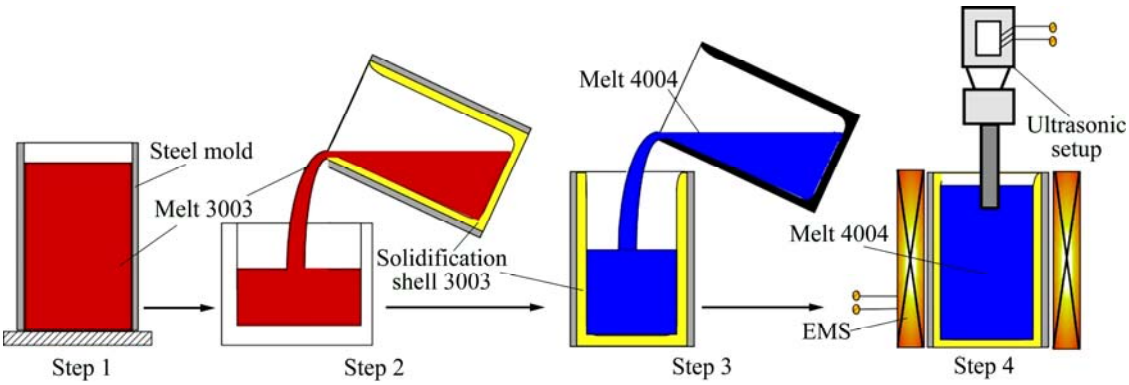


**Fig. 1** Schematic diagram of this experimental procedure

**Table 2** Experimental parameters

| Ultrasonic power/W | Ultrasonic frequency/ kHz | Inserted depth of ultrasonic probe/m | Exciting voltage/ V | Temperature of 3003 alloy solidification shell/K | Pouring temperature of 4004 alloy/K | Physical field treated temperature/K |
|---|---|---|---|---|---|---|
| 200 | 22.5 | 0.01 | 80 | 673 | 967 | 957 |

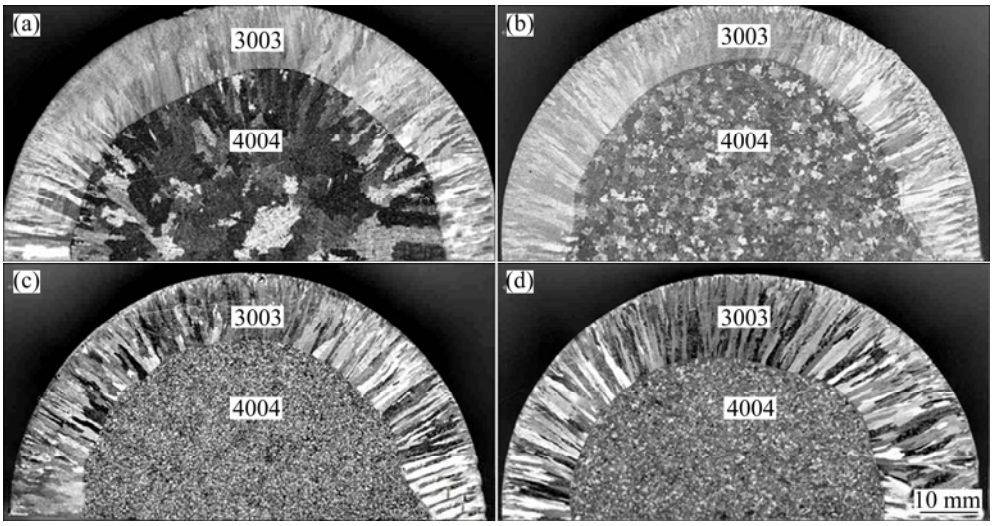


**Fig. 2** Macrostructures of 3003/4004 clad ingots solidified under diverse physical fields: (a) Without external physical field; (b) With electromagnetic stirring; (c) With power ultrasonic; (d) With compound field

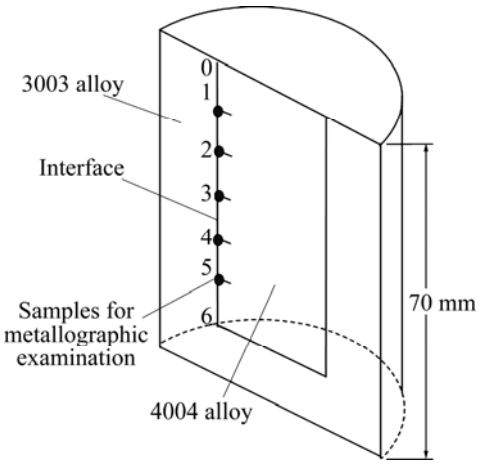


**Fig. 3** Sampling positions for microstructure observation in clad ingot

Figure 4(a) shows the solidification structure at the interface of 3003/4004 clad ingot without any treatment. It can be seen that the typical dendritic crystals grow from the 3003 alloy side towards the 4004 alloy side, and the coarse acicular eutectic silicon disperses among these dendrites. Figure 4(b) presents the solidification structure of the ingot with electromagnetic stirring (ESM). The primary $\alpha$(Al) changes from dendrite grains to irregular fine grains. When the melt is treated by power ultrasonic (UST), the solidification structure of inner 4004 alloy changes from dendritic grains to globular grains, and the average grain size reduces to 110 μm, as shown in Fig. 4(c). Figure 4(d) displays the solidification structure under the compound physical field of power ultrasonic and electromagnetic stirring (UE). The results indicate that there are not only globular grains but also irregular petal-like grains, and the average grain size is 112 μm, showing that the refinement effect is nearly the same with the sample treated by sole power ultrasonic. The average size of primary $\alpha$(Al) is shown in Fig. 5.

In general, during the solidification of inner layer 4004 alloy melt, as a substrate of 3003 solidification shell, 4004 alloy will nucleate and form dendrites growing parallel to heat flow but opposite direction, as shown in Fig. 4(a). In the case of electromagnetic stirring, under the effect of forced convection caused by magnetic force, the secondary dendritic arms may separate from the primary dendrites, resulting in a structural transformation from dendrites to irregular fine grains [9]. It is well known that when power ultrasonic is injected into the melt, a series of unique phenomena occur such as cavitation and acoustical stream. Both of the two effects may contribute to the refinement of the solidification structure. However, according to the available literatures [10−12], the dominant mechanism for grain refinement of power ultrasonic is cavitation-induced heterogeneous nucleation. However, the forced convection resulted from electromagnetic stirring and ultrasonic acoustical stream is beneficial to the bulk distribution of refined grains in the whole ingot. When ultrasonic spreads in aluminum melt, sound waves are damped by the energy absorbance in liquids. The intensity of power ultrasonic at a distance of $X$ from the sound source $I_X$ can be described as follows [13]:

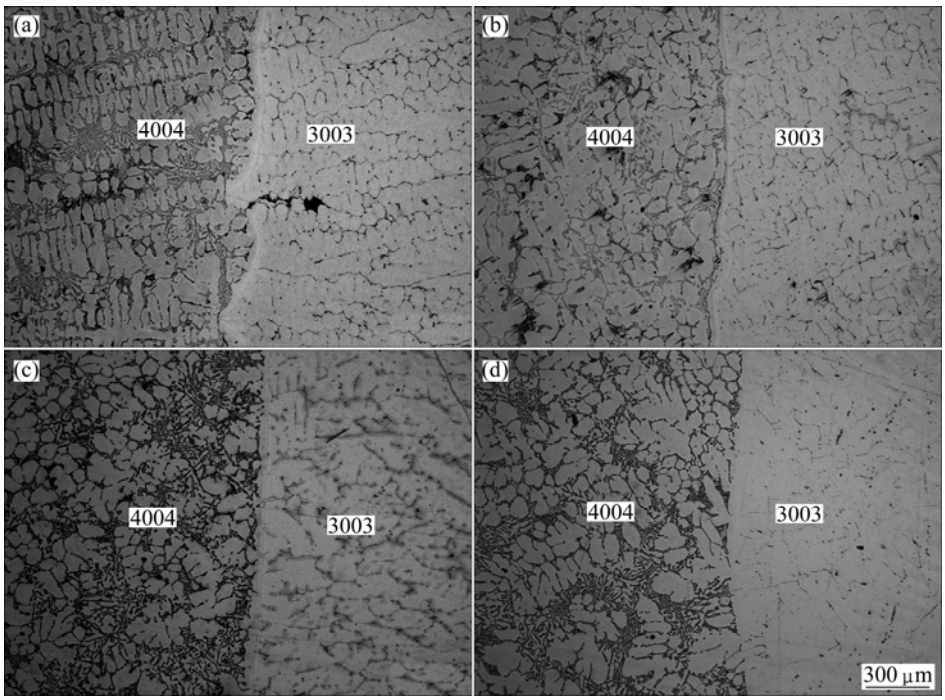


**Fig. 4** Optical microstructures of interface region in clad ingots: (a) Without external physical field; (b) With electromagnetic stirring; (c) With power ultrasonic; (d) With compound field

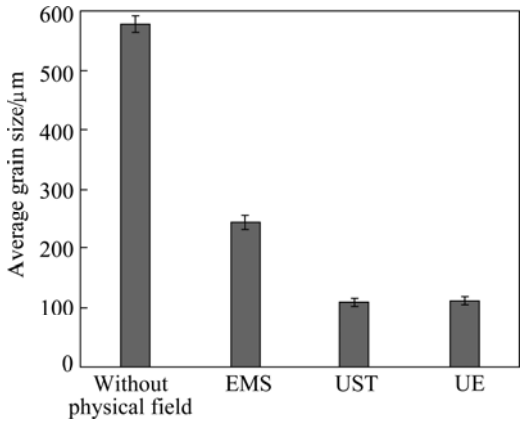


**Fig. 5** Average grain size of primary $\alpha$(Al) in 4004 alloy under diverse physical fields

$$I_X = I_0 \exp(-2\alpha X) \tag{1}$$

where $I_0$ is the intensity at the sound source and $\alpha$ is the attenuation constant.

$$\alpha = \frac{\omega^2 \eta}{2\rho c^3} \tag{2}$$

$$\eta = \eta_0 \exp[E/(RT)] \tag{3}$$

where $\omega$ is the angular frequency, $\rho$ is the density of melt, $\eta_0$ is the viscosity, $c$ is the acoustic velocity and $\eta$ is the viscosity of melt at temperature $T$.

Combining Eqs. (1)−(3), we can obtain the relation between effect distance of ultrasonic and the temperature of melt.

$$X = -\frac{\ln I_0}{\ln I_X} \frac{\omega^2 \eta_0 \exp[E/(RT)]}{\rho c} \tag{4}$$

According to Eq. (1), it is noted that the acoustic intensity is in inverse proportion to the distance from the sound source. So, if the size of ingot is too large, the ultrasonic intensity in the region far away from the sound source will be very low. At the same time, from Eq. (4), it can be seen that the effect distance of ultrasonic decreases with decreasing temperature of the melt.

As reported by LIU [14], for Al−7.3%Si, 20 mm away from the sound source the attenuation is about 41 dB at 850 K, and 60 mm away from the sound source is about 47 dB at 850 K. The results indicate that the attenuation is heavier during the solidification of melt. The attenuation results in the decrease of refinement effect in the region far away from the sound source.

However, the melt treated by electromagnetic stirring, the forced convection in bulk area caused by magnetic force can transfer the cavitation-induced nucleuses into the region far away the sound source. Therefore, the compound field of power ultrasonic and electromagnetic stirring is good for the uniform distribution of refined grains. For the ingot with a large size, the superiority of compound field will be obvious.

### 3.2 Effect of physical fields on Si morphology at interface of clad ingots

Figure 6 presents the typical Si morphology of

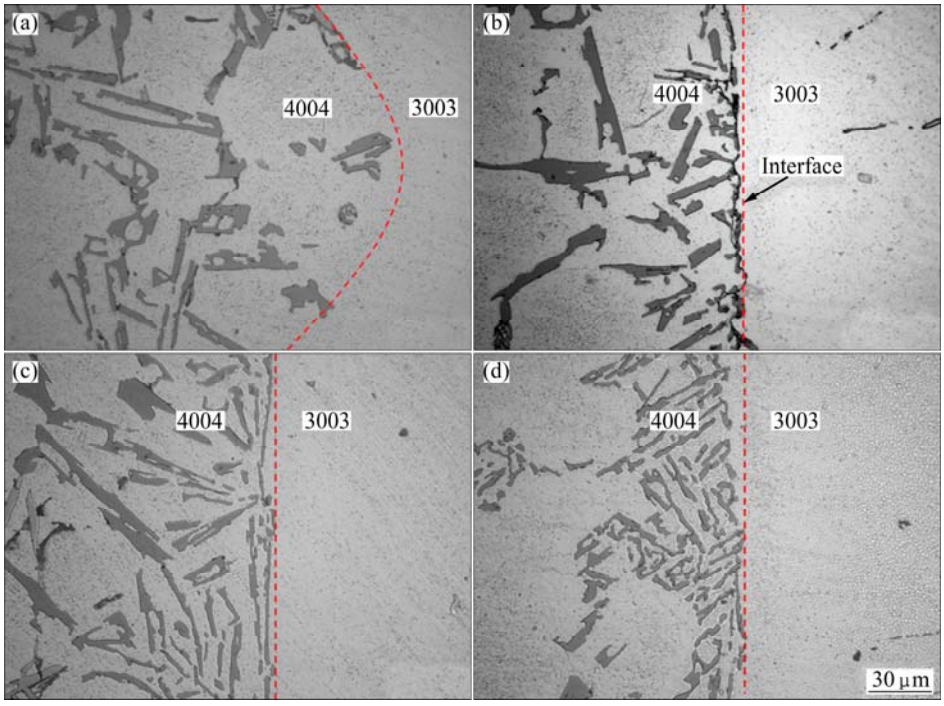


**Fig. 6** Eutectic Si morphologies near interface of clad ingots: (a) Without external physical fields; (b) With electromagnetic field; (c) With power ultrasonic; (d) With compound field

position 3 in Fig. 3 near the interface of 3003/4004 ingots treated by diverse physical fields. For the ingot without any external physical field, coarse eutectic silicon disperses in the primary $\alpha$(Al), as shown in Fig. 6(a). While the electromagnetic stirring is imposed, the morphology of eutectic silicon is still coarse plate-like, as presented in Fig. 6(b). The average width of ingots with power ultrasonic decreases and the morphology changes into thin acicular from a coarse plate-like form. Further, when the two physical fields are unitedly imposed into the melt, the compound effect of power ultrasonic and electromagnetic field results in a from coarse plate-like to fine coral-like form in the eutectic silicon morphology, as presented in Fig. 6(d).

Figure 7 shows the results of quantitative metallographic analysis of silicon morphology. Without any treatment, the average length of eutectic silicon is 48 μm and the average width is 10 μm. While with the electromagnetic stirring treatment, the eutectic silicon is about 50 μm in length, and 8 μm in width. With the ultrasonic treatment, the morphology of Si grain is modified to thin acicular-like from coarse plate-like form, the average length of eutectic silicon decreases to 30 μm and the average width is 2.5 μm, while with the compound field, the average size of eutectic silicon is about 12 μm in length, and 2 μm in width.

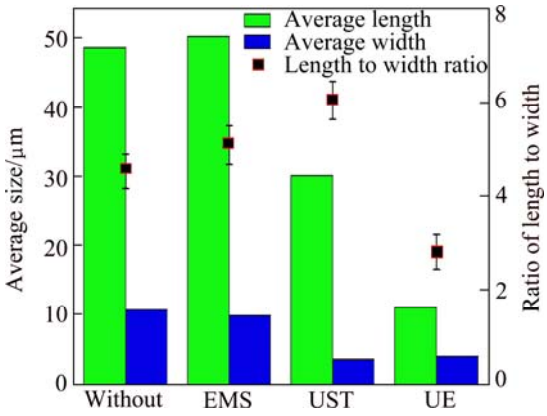


**Fig. 7** Eutectic Si morphological analyses of 4004 alloy under diverse physical fields

Under the effect of forced convection caused by magnetic force, the movement of liquid around growing silicon flakes induced bending stress causes fracture in the silicon which has a very little strength [15]. The broken silicon flakes are transferred into other parts of the liquid and become gradually thick and broad, as shown in Fig. 6(b).

The eutectic Si in hypoeutectic Al−Si alloys nucleates on the impurity-based particles before the eutectic reaction [16]. Ultrasonic cavitation can induce pressure fluctuation in the melt and increase the wettability between impurity particles and melt [17] which is advantageous to the nucleation of eutectic Si on these impurity particles or primary $\alpha$(Al) grains [18]. In addition, acoustically induced convection can also affect nucleation of the silicon phases by altering the constitutional supercooling at the front of the growing eutectic grains [18,19]. Therefore, the average width decreases and the morphology changes to thin acicular from a coarse plate-like form. Under the compound field, the forced convection caused by magnetic force and acoustic stream will be enhanced. The thin acicular silicon resulted from power ultrasonic will easily fracture. The broken silicon flakes increase, therefore, the morphology of eutectic silicon is modified from a coarse plate-like form to a finely short stick form.

As discussed in section 3.1, for the primary $\alpha$(Al), the refinement effect by compound field is nearly the same with that treated by sole power ultrasonic. However, the compound field has more obvious refined effect on the eutectic silicon. When the compound field is applied to the melt, the turbulence of the melt and heat effect both increase. For the small inner layer ingot (40 mm in diameter, 60 mm in height), the solidification time will be longer than that of the sole power ultrasonic. Therefore, the refinement effect of $\alpha$(Al) by compound field is weakened due to the grain growth. However, the ultrasonic cavitation and enhanced convection during the prolonged solidification process are more beneficial to break the growing silicon, resulting in the more obvious refinement of eutectic Si, as shown in Fig. 6.

## 4 Conclusions

1) When the clad ingot is treated by electromagnetic stirring, the solidification structure of inner layer 4004 alloy changes from dendritic-like crystals to petal-like grains.

2) Under the effect of power ultrasonic, the solidification microstructure of 4004 alloy exhibits the refinement of both primary $\alpha$(Al) and eutectic silicon.

3) Under the compound field, the primary $\alpha$(Al) is refined and the morphology of eutectic silicon has a transition from a coarse acicular plate-like form without treatment or thin acicular-like form with power ultrasonic to fine coral-like form.

## References

[1] MILLER W S, ZHUANG L, BOTTEMA J, WITTEBROOD A J, P De SMET, HASZLER A. Recent development in aluminum alloys for the automotive industry [J]. Mater Sci Eng A, 2000, 280: 37−49.

[2] MANESH H D, TAHERI A K. An investigation of deformation

behavior and bonding strength of bimetal strip during rolling [J]. Mech Mater, 2005, 37: 531−542.
[3] KACAR R, ACARER M. An investigation on the explosive clad of 316L stainless steel-din-P355GH steel [J]. J Mater Process Technol, 2004, 152: 91−96.
[4] YILMAZ O, ÇELIK H. Electrical and thermal properties of the interface at diffusion-bonded and soldered 304 stainless steel and copper bimetal [J]. J Mater Process Technol, 2003, 141: 67−76.
[5] KAZANOWSHI P, EPLER M E, MISIOLEK W Z. Bimetal rod extrusion-process and product optimization [J]. Mater Sci Eng A, 2004, 369: 170−180.
[6] FU D F, NING H L, CHEN Z H. Spray deposition technology and preparation of bi-metals [J]. Ordnance Mater Sci Eng A, 2001, 24(1): 65−67.
[7] WANG Tong-min, LI Jun, DU Yan-yan, YAN Zhi-ming, SUN Jian-bo, CAI Shao-wu, XU Jing-jing, LI Ting-ju. Study on continuous casting of clad aluminium alloys with electromagnetic brake [J]. Mater Res Innov, 2010, 14(4): 271−276.
[8] SUN Jian-bo, SONG Xiao-yang, WANG Tong-min, YU Ying-shui, SUN Min, CAO Zhi-qiang, LI Ting-ju. The microstructure and property of Al−Si alloy and Al−Mn alloy bimetal prepared by continuous casting [J]. Materials Letters, 2012, 67: 21−23.
[9] NAFISI S, EMADI D, SHEHATA M T, GHOMASHCHI R. Effects of electromagnetic stirring and superheat on the microstructural characteristics of Al−Si−Fe alloy [J]. Mater Sci Eng A, 2006, 432: 71−83.
[10] FU Y, LI T J. Effect of ultrasonic treatment on solidification structure of 3003/4004 clad ingots [J]. Materials Technology, 2012, 27: 176−179.
[11] JIAN X, MEEK T T, HAN Q. Refinement of eutectic silicon phase of aluminum A356 alloy using high-intensity ultrasonic vibration [J]. Scripta Materialia, 2006, 54: 893−896.
[12] LI X T, LI T J, LI X M, JIN J Z. Study of ultrasonic melt treatment on the quality of horizontal continuously cast Al−1%Si alloy [J]. Ultrason Sonochem, 2006, 13: 121−125.
[13] KOBAYASHI M, KAMATA C, KIMIHISA I T O. Cold model experiments of gas removal from molten metal by an irradiation of ultrasonic waves [J]. ISIJ International, 1997, 37: 9−15.
[14] LIU Qing-mei. Research of ultrasonic treatment on solidification characteristics and structure of metal [D]. Shanghai: University of Shanghai, 2007: 102−106. (in Chinese)
[15] KOCATEPE K, BURDETT C F. Effect of low frequency vibration on macro and micro structures of LM6 alloys [J]. Journal of Materials Science, 2000, 35: 3327−3335.
[16] SHANKAR S, RIDDLE Y W, MAKHLOUF M M. Nucleation mechanism of the eutectic phases in aluminum silicon hypoeutectic alloys [J]. Acta Mater, 2004, 52: 4447−4460.
[17] ESKIN G I. Ultrasonic treatment of light alloy melts [M]. Amsterdam: Gordon and Breach Science Publishers, 1998: 1−25.
[18] ZHANG Z T, LI J, YUE H Y, ZHANG J, LI T J. Microstructure evolution of A365 alloy under compound field [J]. J Alloys Compd, 2009, 484: 458−462.
[19] LI Jun-wen, MOMONO T, FU Ying, JIA Zheng, TAYU Y. Effect of ultrasonic stirring on the temperature distribution and grain refinement in an Al−1.65wt.% Si alloy melt [J]. Transactions of Nonferrous Metals Society of China, 2007, 17(4): 691−697.

# 物理场对 3003/4004 复合铸锭凝固组织的影响

付 莹，接金川，张宇博，钟德水，李继展，李廷举

大连理工大学 材料科学与工程学院，大连 116024

**摘 要**：采用电磁搅拌、功率超声、超声电磁复合场等不同物理场制备 3003/4004 铝合金复合铸锭。结果表明，在电磁搅拌作用下，界面附近 4004 合金一侧 $\alpha$(Al)组织从未施加外场的树枝状转变为花瓣状。在功率超声作用下，4004 合金中 $\alpha$(Al)及共晶硅组织都得到了良好的细化。在超声和电磁场联合作用下，界面处 4004 合金中的 $\alpha$(Al)组织同样得到细化，并且界面处的共晶硅组织较单独超声铸锭的更细小，其形貌从未施加外场时的粗大板条状及施加超声后的细针状转变为细小短棒状。

**关键词**：铝合金；复合铸锭；功率超声；电磁搅拌；复合场；组织

**(Edited by Xiang-qun LI)**